Synthesis and Structural Characterization of Tetranuclear, Bimetallic Sulfido Nitrosyl and Carbonyl Clusters of the Type $Cp_2M_2M'_2S_{3,4}L_n$ (M = Mo, W; M′ = Fe, Co; L = NO, CO)

M. Adnan Mansour, M. David Curtis,* and Jeff W. Kampf

Department of Chemistry, The Willard H. Dow Laboratory, The University of Michigan, Ann Arbor, Michigan 48109-1055

Received August 22, 1996[⊗]

A series of new bimetallic sulfido clusters, $Cp^{\#}{}_2M_2M'_2S_4(NO)_2$ ($Cp^{\#} = C_5Me_2Et$, C_5Me_5, C_5H_5; M = Mo, W; M′ = Fe, Co) have been synthesized and characterized by X-ray diffraction. Two new tungsten carbonyl clusters, $Cp^*{}_2W_2Co_2S_4(CO)_2$ and $Cp^{Et}{}_2W_2Co_2S_3(CO)_5$, were also synthesized and the structure of the latter determined. The structural systematics are related to the redox properties and to the electronic structure of the clusters.

Introduction

In recent years, the chemistry of transition-metal cluster complexes has focused on their potential applications as models for catalytic systems, as catalyst precursors, or as catalysts themselves.[1] Heterobimetallic sulfido clusters have special interest as synthetic analogs of such diverse materials as biological enzymes, *e.g.* nitrogenases[2] and hydrogenases,[3] and industrial heterogeneous catalysts, *e.g.* those used for hydrodesulfurization (HDS).[4] The HDS catalyst consists of molybdenum sulfide supported on high-surface-area alumina and "promoted" with cobalt sulfide, which forms an intimate phase with the molybdenum sulfide.[4a,b] We have previously shown that organometallic Mo/Co/S clusters in solution mimic many aspects of the desulfurization activity of these heterogeneous catalysts and that these clusters also form the catalytically active site when adsorbed onto alumina.[4c,5]

Riaz et al.[5b] have shown that $Cp'_2Mo_2Co_2S_3(CO)_4$ (**1**), a 60-VSE (VSE = valence shell electron), electronically unsaturated cluster, reacts with many different organic sulfur compounds to give a single organometallic product, the cubane cluster $Cp'_2Mo_2Co_2S_4(CO)_2$ (**2′**), in near-quantitative yield, along with the corresponding desulfurized hydrocarbon. Cluster **2′** is a 60-VSE, electron precise cluster. Druker and Curtis[5c] reported a kinetic study of the reactions of thiols and thiolates of alkanes and arenes with cluster **1** and demonstrated that the coordination of thiols and thiolates to cluster **1** activates the C−S bond toward homolysis. These studies showed that the value of $\Delta H^{\ddagger}$ for the C−S cleavage process mediated by cluster **1** has a value nearly 75% lower than that of the free thiol. We have also shown that the cluster $Cp^{Et}{}_2Mo_2Co_2S_4(CO)_2$ (**2**), where $Cp^{Et} = C_5Me_4Et$, is capable of abstracting sulfur from small-ring cyclic sulfides and PhSH.[5a]

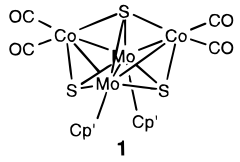

1

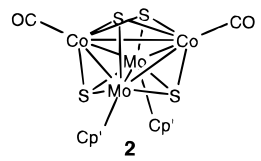

2

The aforementioned kinetic studies showed that the slow step in the desufurization of arene thiols was the initial coordination of the thiol to the electronically unsaturated cluster **1**. The questions arise, then, as to whether or not the electronic unsaturation of the cluster itself is the determining factor in the observed reactivity, whether or not the Co atom is playing a special role in the desulfurization reactions, and if the electrophilicity of the clusters were enhanced, would the desulfurization activity be enhanced? To help address these questions, we have synthesized a series of new heterobimetallic sulfido clusters which resemble cluster **1** or **2** structurally but differ in metal composition and electron count and have carbonyl ligands replaced with the more electron-withdrawing nitrosyl ligand.

Several strategies may be used in the preparation of clusters with heteronuclear metal−metal bonds, and these have been well reviewed.[6−12] A rational methodology for the preparation of heterobimetallic sulfido

[⊗] Abstract published in *Advance ACS Abstracts,* January 1, 1997.

(1) Gates, B. C., Guczi, L., Knozinger, H., Eds. *Metal Clusters in Catalysis*; Elsevier: New York, 1986.

(2) (a) Holm, R. H. *Adv. Inorg. Chem.* **1992**, *38*, 1 and references therein. (b) Coucouvanis, D. *Acc. Chem. Res.* **1991**, *24*, 1. (c) Burgess, B. K. *Chem. Rev.* **1990**, *90*, 1377. d) Holm, R. H.; Simhon, E. D. In *Molybdenum Enzymes*; Spiro, T. G., Ed.; Wiley-Interscience: New York, 1985; Chapter 1.

(3) (a) Tan, G. O.; Ensign, S. A.; Cuirli, S.; Scott, M. J.; Hedman, B.; Holm, R. H.; Ludden, P. W.; Korszun, Z. R.; Stephens, P. J.; Hodgson, K. O. *Proc. Natl. Acad. Sci. U.S.A.* **1992**, *89*, 4427. (b) Bridya, N.; Olmstead, M. M.; Whitehead, J. P.; Bagyinka, C.; Maroney, M. J.; Mascharak, P. K. *Inorg. Chem.* **1992**, *31*, 3612. (c) Zhou, J.; Scott, M. J.; Hu, Z.; Peng, G.; Munck, E.; Holm, R. H. *J. Am. Chem. Soc.* **1992**, *114*, 10843.

(4) (a) Chianelli, R. R.; Daage, M.; Ledoux, M. J. *Adv. Catal.* **1994**, *40*, 177. (b) Topsøe, H.; Clausen, B. S.; Massoth, F. E. In *Catalysis-Science and Technology*; Anderson, J. R., Boudart, M., Eds.; Springer-Verlag: New York, 1996; Vol. 11. (c) Curtis, M. D.; Penner-Hahn, J. E.; Schwank, J.; Baralt, O.; McCabe, D.; Thompson, L.; Waldo, G. *Polyhedron* **1988**, *7*, 2411. (d) Coucouvanis, D.; Hadjikyriacou, A.; Draganjac, M.; Kanatzidis, M. G.; Ileperuma, O. *Polyhedron* **1986**, *5*, 349. (e) Draganjac, M.; Rauchfuss, T. B. *Angew. Chem., Int. Ed. Engl.* **1985**, *24*, 742. (f) Dubois, M. R. *J. Am. Chem. Soc.* **1983**, *105*, 3170.

(5) (a) Mansour, M. A.; Curtis, M. D.; Kampf, J. W. *Organometallics* **1995**, *14*, 5460. (b) Druker, S. H.; Curtis, M. D. *J. Am. Chem. Soc.* **1995**, *117*, 6366. (c) Riaz, U.; Curnow, O. J.; Curtis, M. D. *J. Am. Chem. Soc.* **1994**, *116*, 4357. (d) Curnow, O. J.; Kampf, J. W.; Curtis, M. D.; Shen, J.-K.; Basolo, F. *J. Am. Chem. Soc.* **1994**, *116*, 224. (e) Curnow, O. J.; Curtis, M. D. *Organometallics* **1994**, *13*, 2489. (f) Curtis, M. D. *Appl. Organomet. Chem.* **1992**, *6*, 429.

S0276-7333(96)00724-8 CCC: $14.00

clusters has been developed in which a bimetallic sulfido precursor with the desired number of sulfur atoms is allowed to react with a late-transition-metal complex which possesses the desired vertex ligands. The strategy involves the expansion of the coordination number of the sulfur ligands (μ_n-S) and has been described previously.[6,13−16] This paper describes the preparation, structures, and electrochemistry of a new series of tetranuclear sulfido clusters.

Experimental Section

All manipulations and reactions were carried out under a dinitrogen atmosphere using standard Schlenk line techniques or in an inert-atmosphere glovebox. Reagent grade solvents were dried and distilled prior to use: toluene from Na/benzophenone, decahydronaphthalene (decalin), dichloromethane, and hexane from CaH_2, and acetonitrile (predried over 3 Å sieves) from B_2O_3. $Cp_2Mo_2(S)_2(\mu\text{-}SH)_2$/$Cp'_2Mo_2(S)_2(\mu\text{-}SH)_2$,[17] $Cp^{Et}{}_2Mo_2S_4$,[18] $Cp^*{}_2W_2S_4$/$Cp^{Et}{}_2W_2S_4$,[18] $Cp^*{}_2W_2S_3(CO)_2$/$Cp^{Et}{}_2W_2S_3(CO)_2$,[18] $Cp^{Et}{}_2Mo_2S_4I_2$[19] (Cp = C_5H_5, Cp′ = C_5H_4Me, Cp* = C_5Me_5, and Cp^{Et} = C_5Me_4Et), $Na[Fe(CO)_3(NO)]$,[20] $Fe(NO)_2(CO)_2$,[21] and $Co(CO)_3(NO)$[22] were prepared according to published procedures or slight adaptations thereof. (Note: In all the following procedures that use $Cp^{\#}{}_2M_2S_4$, the "as prepared" mixture of isomers was used. It was established that the different isomers gave the same products in these reactions.) All other reagents were used as purchased from Aldrich Chemical Company or Strem Chemical, Inc.

^{1}H NMR spectra were collected on a Bruker AM-360, AM-300, or AM-200 spectrometer and referenced to the residual proton solvent resonance. FT-IR spectra were collected on a Nicolet 5-DXB spectrometer, and the spectra were corrected for background and solvent effects. Mass spectra were collected on a VG 70-250-S high-resolution spectrometer. The molecular ion peaks reported correspond to the most intense peak in a polyisotopic pattern. Cyclic voltammetry (CV) was run using a Princeton Applied Research Model 173 potentiostat. The voltage was generated by a digital-to-analog converter on a National Instruments Model AT-MIO-16E-10 data acquisition card. The current was digitized by the analog-to-digital converter on the same card. Acquisition commands and data workup were controlled by a custom-written software package.[23] Elemental analyses were performed by the Microanalysis Laboratory at The University of Michigan.

Preparation of $Cp^{Et}{}_2Mo_2Fe_2S_4(NO)_2$ (3a). (a) In the glovebox, a 100 mL Schlenk flask was charged with $Na[Fe(CO)_3(NO)]$ (0.029 g, 0.1504 mmol) and then removed from the box and attached to a Schlenk line. To this solid was added $Cp^{Et}{}_2Mo_2S_4I_2$ (0.079 g, 0.10 mmol). The flask was then evacuated and back-filled with N_2 (2×). To the mixture was added THF (40 mL) to give a yellow-brown solution, which was stirred at room temperature. After 30 min, the solution had become dark orange-brown. Chromatographic workup on a silica gel column (25 × 3 cm) using a mixture of toluene/hexane (1:1) as eluent gave an orange band, which was collected first. A second, green/black band did not elute down the column using toluene as eluent. The orange solution was concentrated *in vacuo* and filtered again through a 3 cm plug of Celite, which was washed with toluene until the washings were colorless. Recrystallization from toluene/hexane (1:4) at −18 °C gave long black platelets, which were isolated from solution and dried *in vacuo*; yield 0.030 g (38%). IR (KBr; cm^{-1}): ν_{NO} 1736 (s) and 1715 (s). ^{1}H NMR (C_6D_6; δ): 0.80 (t), $CpCH_2CH_3$; 1.64 (s) and 1.69 (s), $CpCH_3$; 2.02 (q), $CpCH_2CH_3$. Anal. Calcd for $Cp^{Et}{}_2Mo_2Fe_2S_4(NO)_2$: C, 33.43; H, 4.34; N, 3.54. Found: C, 33.56; H, 4.16; N, 3.63.

(b) A 100 mL Schlenk flask was charged with $Cp^{Et}{}_2Mo_2S_4$ (0.081 g, 0.131 mmol), and this compound was dissolved in toluene (∼30 mL). To this solution was added $Fe(NO)_2(CO)_2$ (0.035 mL, 0.32 mmol), *via* syringe. The reaction mixture was heated at reflux for 2 h, cooled to room temperature, and then filtered through a 2 cm plug of Celite, which was washed with toluene until the washings were colorless. Recrystallization from toluene/hexane (1:3) at −18 °C gave a black crystalline solid, which was isolated from solution and dried *in vacuo*; yield 0.043 g (41%). IR (KBr, cm^{-1}): ν_{NO} 1736 (s) and 1715 (s). ^{1}H NMR ($CDCl_3$; δ): 1.07 (t), $CpCH_2CH_3$; 1.97 (s), $CpCH_3$; 1.98 (s), $CpCH_3$; 2.22 (q), $CpCH_2CH_3$. Anal. Calcd for $Cp^{Et}{}_2Mo_2Fe_2S_4(NO)_2$: C, 33.43; H, 4.34; N, 3.55. Found: C, 33.73; H, 4.32; N, 3.55.

Preparation of $Cp_2Mo_2Fe_2S_4(NO)_2$ (3b). The same procedure as that for the preparation of **3a**, part b, was followed, except the Mo/S synthon used was $Cp_2Mo_2S_2(\mu\text{-}SH)_2$ (0.098 g, 0.216 mmol). Recrystallization from toluene/hexane (1:4) at −18 °C gave a black microcrystalline solid, which was isolated from solution and dried *in vacuo*; yield 51 mg (37%). IR (KBr, cm^{-1}): ν_{NO} 1734 (s) and 1715 (vs). ^{1}H NMR ($CDCl_3$): δ 5.69 (s). Anal. Calcd for $Cp_2Mo_2Fe_2S_4(NO)_2$: C, 19.31; H, 1.62; N, 4.50. Found: C, 18.82; H, 1.69; N, 5.20.

Preparation of $Cp^{Et}{}_2Mo_2Co_2S_4(NO)_2$ (4a). $Co(CO)_3(NO)$ (0.104 g, 0.60 mmol) was transferred to a tared 100 mL Schlenk flask *via* trap-to-trap distillation. Then, the $Co(CO)_3(NO)$ was dissolved in toluene (20 mL) and the solution was subsequently added to a yellow-brown solution of $Cp^{Et}{}_2Mo_2S_4$ (0.180 g, 0.291 mmol) in toluene (20 mL). The reaction mixture was heated to reflux for 30 min, allowed to cool to room temperature, and then filtered through a 4 cm plug of Celite, which was washed with toluene until the washings were colorless. Recrystallization from toluene/hexane (1:5) at −18 °C gave black platelets, which were isolated from solution

(6) (a) Curtis, M. D.; Riaz, U.; Curnow, O. J.; Kampf, J. W.; Rheingold, A. L.; Haggerty, B. S. *Organometallics* **1995**, *14*, 5337. (b) Li, P.; Curtis, M. D. *Inorg. Chem.* **1990**, *29*, 1242. (c) Curtis, M. D.; Williams, P. D.; Butler, W. M. *Inorg. Chem.* **1988**, *27*, 2853.

(7) (a) Adams, R. D. In *Comprehensive Organometallic Chemistry II*; Abel, E. W., Stone, F. G. A., Wilkinson, G., Eds.; Pergamon: Oxford, U.K., 1995; Vol. 10, Chapter 1, p 1. (b) Roberts, D. A.; Geoffroy, G. L. In *Comprehensive Organometallic Chemistry I*; Wilkinson, G., Stone, F. G. A., Abel, E. W., Eds.; Pergamon: Oxford, U.K., 1982; Vol. 6, Chapter 40, p 763.

(8) Vahrenkamp, H. *Adv. Organomet. Chem.* **1983**, *22*, 169.

(9) Farrugia, L. J. *Adv. Organomet. Chem.* **1990**, *31*, 301.

(10) Sappa, E.; Tiripicchio, A.; Braunstein, P. *Chem. Rev.* **1983**, *83*, 203.

(11) Stone, F. G. A. *Pure Appl. Chem.* **1986**, *58*, 529.

(12) Braunstein, P. In *Perspectives in Coordination Chemistry*; Williams, A. F., Floriani, C., Merbach, A. E., Eds.; Verlag Helvetica Chimica Acta: Basel, Switzerland, 1992; p 67.

(13) (a) Brunner, H.; Grass, R.; Wachter, J.; Nuber, B.; Zeigler, M. L. *J. Organomet. Chem.* **1990**, *393*, 119. (b) Brunner, H.; Janietz, N.; Wachter, J.; Zahn, T.; Zeigler, M. L. *Angew. Chem., Int. Ed. Engl.* **1985**, *24*, 133. (c) Brunner, H.; Kauermann, H.; Wachter, J. *J. Organomet. Chem.* **1984**, *265*, 189. (d) Brunner, H.; Kauermann, H.; Wachter, J. *Angew. Chem., Int. Ed. Engl.* **1983**, *22*, 549. (e) Brunner, H.; Wachter, J. *J. Organomet. Chem.* **1982**, *240*, C41.

(14) (a) Rauchfuss, T. B.; Gammon, S. D.; Weatherill, T. D.; Wilson, S. R. *New J. Chem.* **1988**, *12*, 373. (b) Rauchfuss, T. B.; Weatherill, T. D.; Wilson, S. R.; Zebrowski, J. P. *J. Am. Chem. Soc.* **1983**, *105*, 6508.

(15) Halbert, T. R.; Cohen, S. A.; Steifel, E. I. *Organometallics* **1985**, *4*, 1689.

(16) Feng, Q.; Rauchfuss, T. B.; Wilson, S. R. *J. Am. Chem. Soc.* **1995**, *117*, 4702.

(17) (a) Curtis, M. D.; Williams, P. D. *Inorg. Chem.* **1983**, *22*, 2661. (b) Kubas, G. J.; Ryan, R. R.; Kubat-Martin, K. A. *J. Am. Chem. Soc.* **1989**, *111*, 7823.

(18) Brunner, H.; Meier, W.; Wachter, J.; Guggolz, E.; Zahn, T.; Zeigler, M. L. *Organometallics* **1982**, *1*, 1107.

(19) Brunner, H.; Meier, W.; Wachter, J.; Weber, P.; Zeigler, M. L.; Enemark, J. H.; Young, C. G. *J. Organomet. Chem.* **1986**, *309*, 313.

(20) Heiber, W.; Beutner, H. *Z. Anorg. Allg. Chem.* **1963**, *101*, 320.

(21) King, R. B. *Organometallic Syntheses*; Academic Press: New York, 1965; Vol. 1, p 167.

(22) Job, R.; Rovang, J. *Synth. React. Inorg. Met.-Org. Chem.* **1976**, *6*, 367.

(23) Parus, S., CV Control and Data Acquisition and Display Program, Department of Chemistry, The University of Michigan, 1995.

and dried *in vacuo*; yield 97 mg (42%). IR (KBr, cm^{-1}): ν_{NO} 1747 (s) and 1717 (s). ^1H NMR ($CDCl_3$; δ): 1.04 (t), $CpCH_2CH_3$; 1.89 (s), $CpCH_3$; 1.92 (s), $CpCH_3$; 2.19 (q), $CpCH_2CH_3$. Anal. Calcd for $Cp^{Et}{}_2Mo_2Co_2S_4(NO)_2$: C, 33.18; H, 4.30; N, 3.52. Found: C, 33.20; H, 4.21; N, 3.58. MS (EI, *m*/*z*): 796 (M^+); 766 ($M^+ - NO$); 736 ($M^+ - 2NO$).

Preparation of $Cp_2Mo_2Co_2S_4(NO)_2$ (4b). The same procedure as that for the preparation of **4a** was followed, except the Mo/S synthon was $Cp_2Mo_2S_2(\mu\text{-}SH)_2$ (0.140 g, 0.329 mmol). Recrystallization from toluene/hexane (1:5) at −18 °C gave a black microcrystalline solid, which was isolated from solution and dried *in vacuo*; yield 62 mg (30%). IR (KBr, cm^{-1}): ν_{NO} 1756 (s) and 1726 (s). ^1H NMR ($CDCl_3$; δ): 4.80 (s). Anal. Calcd for $Cp_2Mo_2Co_2S_4(NO)_2$: C, 19.12; H, 1.60; N, 4.46. Found: C, 19.92; H, 2.07; N, 3.95. MS (EI, *m*/*z*): 628 (M^+); 598 ($M^+ - NO$); 568 ($M^+ - 2NO$); 503 ($M^+ - 2NO - Cp$).

Preparation of $Cp^*{}_2W_2Fe_2S_4(NO)_2$ (5). A 100 mL Schlenk flask was charged with $Cp^*{}_2W_2S_4$ (0.101 g, 0.132 mmol), and this compound was dissolved in toluene (30 mL). To this solution was added $Fe(NO)_2(CO)_2$ (0.040 mL, 0.36 mmol) *via* syringe. The reaction mixture was heated at reflux for 3 h, at which point solution IR indicated ν_{NO} 1726 and 1710 cm^{-1}. The reaction mixture was cooled to room temperature and then filtered through a 3 cm plug of Celite, which was washed with toluene until the washings were colorless. Recrystallization from toluene/hexane (2:3) at −18 °C gave a black crystalline solid, which was isolated from solution and dried *in vacuo*; yield 0.049 g (35.6%). IR (KBr, cm^{-1}): ν_{NO} 1725 (s) and 1699 (s). ^1H NMR ($CDCl_3$): δ 2.23 (s). Anal. Calcd for $Cp^*{}_2W_2Fe_2S_4(NO)_2$: C, 25.61; H, 3.22; N, 2.99. Found: C, 23.62; H, 3.14; N, 3.03. MS (EI, *m*/*z*): 938 (M^+); 908 ($M^+ - NO$); 878 ($M^+ - 2NO$).

Preparation of $Cp^*{}_2W_2Co_2S_4(NO)_2$ (6). $Co(CO)_3(NO)$ (0.23 g, 1.33 mmol) was transferred to a tared 100 mL Schlenk flask *via* trap-to-trap distillation. Then, it was dissolved in toluene (20 mL) and the solution was subsequently added to a yellow-brown solution of $Cp^*{}_2W_2S_4$ (0.340 g, 0.444 mmol) in toluene (30 mL). The reaction mixture was heated to reflux for 2 h, at which point the color had become green-brown and solution IR revealed ν_{NO} 1740 and 1722 cm^{-1}. The reaction mixture was cooled to room temperature, and then it was filtered through a 4 cm plug of Celite, which was washed with toluene until the washings were colorless. Recrystallization from toluene/hexane (1:2) at −18 °C gave a black crystalline solid, which was isolated from solution and dried *in vacuo*; yield 62 mg (30%). IR (KBr, cm^{-1}): ν_{NO} 1732 (s) and 1709 (s). ^1H NMR ($CDCl_3$): δ 2.09 (s). Anal. Calcd for $Cp^*{}_2W_2Co_2S_4(NO)_2$: C, 25.44; H, 3.20; N, 2.97. Found: C, 25.49; H, 3.20; N, 2.99. MS (EI, *m*/*z*): 944 (M^+); 914 ($M^+ - NO$); 884 ($M^+ - 2NO$).

Preparation of $Cp^*{}_2W_2Co_2S_4(CO)_2$ (7). A 100 mL Schlenk flask was charged with $Cp^*{}_2W_2S_4$ (0.102 g, 0.133 mmol). To this was added a solution of $Co_2(CO)_8$ (0.052 g, 0.152 mmol) in toluene (30 mL). The reaction mixture was stirred at room temperature for 2 h, at which point the solution had become yellow-brown. The reaction mixture was filtered through a 5 cm plug of Celite, which was washed with toluene until the washings were colorless. Recrystallization from toluene/hexane (1:2) at −18 °C gave a black crystalline solid, which was isolated from solution and dried *in vacuo*; yield 64 mg (51%). IR (toluene, cm^{-1}): ν_{CO} 1964 and 1946. IR (KBr, cm^{-1}): ν_{CO} 1959 and 1934. ^1H NMR ($CDCl_3$; δ): 2.13 (s). Anal. Calcd for $C_{22}H_{30}W_2Co_2S_4O_2$: C, 28.10; H, 3.22. Found: C, 27.30; H, 3.36.

Preparation of $Cp^{Et}{}_2W_2Co_2S_3(CO)_5$ (8). A 100 mL Schlenk flask was charged with $Cp^{Et}{}_2W_2S_3(CO)_2$ (0.135 g, 0.165 mmol). To this was added a solution of $Co_2(CO)_8$ (0.062 g, 0.181 mmol) in toluene (30 mL). The green-brown reaction mixture was stirred at room temperature for 3 h, at which point the color had become yellow-brown. The reaction mixture was stripped of solvent, the residue was dried *in vacuo* and redissolved in CH_3CN, and this solution was filtered through a 4 cm plug of Celite, which was washed with CH_3CN until the washings were colorless. The filtrate was concentrated to 10 mL and cooled to −4 °C for 20 h to give a black crystalline solid, which was isolated from solution and dried *in vacuo*; yield 69 mg (41%). IR (KBr, cm^{-1}): $\nu_{(Co)CO}$ 2005 (s), 1981 (vs), 1950 (s); $\nu_{(W)CO}$ 1924 (sh). ^1H NMR (C_6D_6; δ): 0.73 (t, 3 H); 0.86 (t, 3 H); 1.78 (overlapping singlets, 12 H); 1.88 (s, 6 H); 1.96 (s, 6 H); 2.22 (q, 2 H); 2.36 (q, 2 H). Anal. Calcd for $Cp^{Et}{}_2W_2Co_2S_3(CO)_5$: C, 31.78; H, 3.36. Found: C, 31.11; H, 3.42. The sample did not maintain its integrity upon ionization for mass spectral analysis.

Cyclic Voltammetry Experiments. The cyclic voltammograms were obtained using a three-electrode cell configuration in a single-compartment cell (20.0 mL capacity). All experiments employed a Pt-disk working electrode in 0.1 M $(TBA)PF_6$ (tetrabutylammonium hexafluorophosphate) in CH_3CN referred to a Ag-wire reference electrode (pseudo-reference), with a Pt-wire auxiliary electrode completing the potentiostatic circuit. The concentration of the cluster of interest was 1 mM or less. Scan rates were varied between 50 and 500 mV/s. Ferrocene was added at the end of each series of runs to provide an internal reference. The ferrocene/ferrocenium (Fc/Fc^+) couple was measured for each sample against the Ag-wire pseudo-reference; corrections were applied to all data according to $(E_{p,a} + E_{p,c})/2 = 400$ mV for the Fc/Fc^+ couple vs NHE.[24]

X-ray Structural Analyses. X-ray Data Collection. Crystallographic data for all X-ray crystal structures can be found in Tables 3 and 4. Black crystals of **3a**, **4a**, **5**, **6**, and **8** were sealed in thin-walled capillaries in air. These crystals were transferred to the cold stream on a Siemens P4u (**3a** and **4a**) equipped with an LT-2 low-temperature device at 178 K or on a Siemens R2m/v (**5**, **6**, and **8**) equipped with an LT-2 low-temperature device at 198 K (**5**), 191 K (**6**), or 178 K (**8**). The unit cell dimensions were obtained from the least-squares fit of 30 reflections ($13.3° \le 2\theta \le 25.0°$) (**3a**), 25 reflections ($2\theta \ge 24°$) (**4a** and **8**), 27 reflections ($2\theta \ge 24°$) (**5**), or 41 reflections ($2\theta \ge 23°$) (**6**). The molecules in **3a**, **4a**, **5**, and **6** each occupy sites of 2-fold symmetry in their respective crystal lattices. In **3a**, the ethyl group of the Cp^{Et} ligand is disordered over two positions, each at 50% occupancy. The 50% hydrogen atoms of these groups were not placed. Three standard reflections, monitored every 97 data points for all structures, showed insignificant variations (<2% for **5** or <3% for **3a**, **4a**, **6**, and **8**). Three reflections with $F^2 < -2\sigma F^2$ (**3a**), ten reflections with $F^2 < -3\sigma F^2$ (**5**), and six reflections with very negative F^2 (**6**) were suppressed in the refinements. An empirical absorption correction (XABS2)[25] (**3a, 4a**, **5**, **6**, and **8**) was applied to the data sets.

Structure Solution and Refinement. The structure for **3a** was solved by direct methods to locate the metal atoms, and the remaining non-hydrogen atoms were located through subsequent difference Fourier synthesis. All non-hydrogen atoms were refined with anisotropic thermal parameters, and all hydrogen atoms were refined isotropically (**3a**). After correction for Lorentz and polarization effects, the structures for **4a**, **5**, **6**, and **8** were solved by standard heavy-atom Patterson techniques followed by weighted Fourier synthesis. Refinement was by full-matrix least-squares techniques based on F^2 to minimize the function $\sum w(|F_o^2 - F_c^2|)^2$ with $w = 1/[\sigma^2(F_o)^2 + (0.077P)^2 + 3.09P]$ (**3a**), $w = 1/[\sigma^2(F_o)^2 + (0.054P)^2 + 1.57P]$ (**4a**), $w = 1/[\sigma^2(F_o)^2 + (0.0604P)^2]$ (**5**), $w = 1/[\sigma^2(F_o)^2 + (0.0335P)^2]$ (**6**), or $w = 1/[\sigma^2(F_o)^2 + (0.0325P)^2]$ (**8**) and $P = [\max(F_o^2,0) + 2F_c^2]/3$. The hydrogen atoms were fit using the Riding model ($d_{C-H} = 0.96$ Å, common U(H)). All calculations for all structures were performed on a VAXStation 3500

(24) (a) Gritzner, G.; Kuta, J. *Pure Appl. Chem.* **1984**, *56*(4), 461. (b) Gagné, R. R.; Koval, C. A.; Lisensky, G. C. *Inorg. Chem.* **1980**, *19*, 2855. (c) Gagné, R. R.; Allison, J. L.; Gall, R. S.; Koval, C. A. *J. Am. Chem. Soc.* **1977**, *99*, 7170.

(25) XABS2, an empirical absorption correction program: Parkin, S.; Moezzi, B.; Hope, H. *J. Appl. Crystallogr.* **1995**, *28*, 53.

Scheme 1

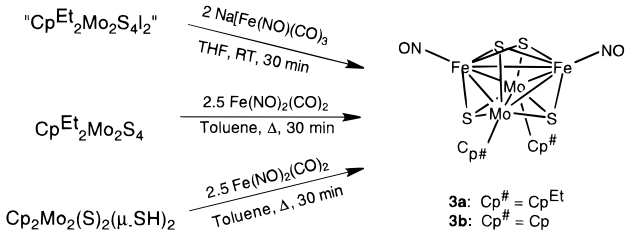

Scheme 2

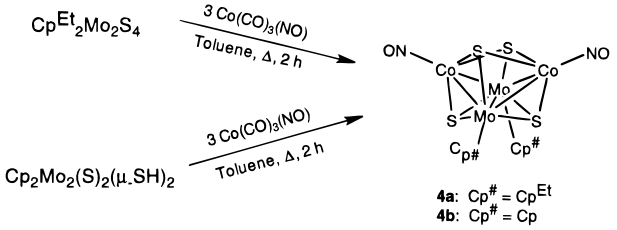

computer using the Siemens SHELXTL PLUS or SHELXL-93 software package[26] (**3a**, **4a**, **5**, **6**, and **8**).

Results and Discussion

Syntheses. The clusters $Cp^{\#}{}_2Mo_2Fe_2S_4(NO)_2$ ($Cp^{\#} = Cp^{Et}$, Cp) were synthesized using different Mo/S cluster synthons and two Fe−nitrosyl complexes as the source of the FeNO vertex, all of which resulted in a product with the same cluster core. In the first case, the product of the reaction of $Cp^{Et}{}_2Mo_2S_4$ with 1 equiv of I_2, to which the formula $[Cp^{Et}{}_2Mo_2S_4]^{2+}I^-{}_2$ has been ascribed by Brunner and co-workers,[19] was prepared. On the basis of this molecular formula, 2 equiv of $Na[Fe(CO)_3NO]$ in THF was added and the reaction was allowed to proceed at room temperature for 30 min (Scheme 1). After purification by column chromatography on silica gel, this cluster was characterized by spectroscopy and by single-crystal X-ray diffraction. The IR spectrum of the cluster $Cp^{Et}{}_2Mo_2Fe_2S_4(NO)_2$ (**3a**) displays NO stretching absorptions at 1736 and 1715 cm^{-1}, and the ^1H NMR spectrum shows the presence of equivalent Cp^{Et} groups. The structure of cluster **3a** is discussed below.

Similarly, the dimer $Cp^{Et}{}_2Mo_2S_4$ was allowed to react in refluxing toluene for 30 min with 2.4 equiv of $Fe(NO)_2(CO)_2$ to give cluster **3a** (Scheme 1). Subsequent to filtration through a plug of Celite, the product was crystallized from a toluene/hexane solvent mixture at −18 °C and was shown spectroscopically to be identical with the product obtained as described above. No reaction was observed at room temperature, and heating the reaction mixture likely results in diminished yields as a result of the degradation of the $Fe(NO)_2(CO)_2$ reagent.

In an analogous reaction, the cluster $Cp_2Mo_2S_2(\mu\text{-}SH)_2$ reacted with a slight excess of $Fe(NO)_2(CO)_2$ in refluxing toluene (Scheme 1) to give a cluster similar to **3a**, with the only difference being the substituents on the cyclopentadienyl ligands (Cp *vs* Cp^{Et}). The cluster $Cp_2Mo_2Fe_2S_4(NO)_2$ (**3b**) displayed NO stretching absorptions at 1734 and 1715 cm^{-1}, and there was a single resonance in the ^1H NMR spectrum at δ 5.69, arising from the equivalent Cp groups. This reaction was attempted in order to obtain a "$Mo_2Fe_2S_3$" cluster analogous to cluster **1**, which was prepared from dicobalt octacarbonyl and the molybdenum sulfhydryl complex $Cp_2Mo_2S_2(SH)_2$.[17a] The formation of a *tri*sulfido Mo/Co cluster was rationalized previously by assuming the facile loss of one S as H_2S under the reaction conditions, but we have no good explanation for why the formation of the Mo/Fe cluster takes a different course.

The synthesis of $Cp^*{}_2Mo_2Fe_2S_4(NO)_2$ was reported by Brunner and co-workers,[13d] although their conditions were different from those described herein. In Brunner's reaction, UV photolysis of the cluster $Cp^*{}_2Mo_2S_4$ in THF in the presence of 2 equiv of $[Ph_3PNPPh_3][Fe(CO)_3(NO)]$ afforded the Cp* analog to cluster **3a**. Although suitable crystals of Brunner's product could not be obtained for X-ray structural determination, it was determined to be analytically pure. The NO absorptions observed by Brunner, ν_{NO} 1734 and 1708 cm^{-1}, are consistent with those we observed for cluster **3a**.

The complex $Cp^*{}_2W_2S_4$ is also prepared readily and has good utility as a cluster synthon. The reaction of $Cp^*{}_2W_2S_4$ with 2.7 equiv of $Fe(NO)_2(CO)_2$ in refluxing toluene for 3 h afforded the W analog of cluster **3a**, $Cp^*{}_2W_2Fe_2S_4(NO)_2$ (**5**) (eq 1). Filtration of the reaction

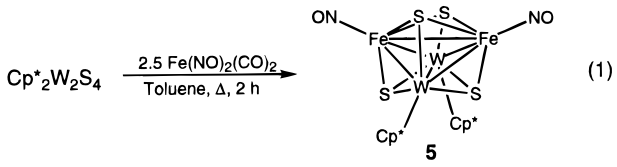

(1)

mixture through Celite, followed by crystallization from a toluene/hexane solvent mixture, gave the product in 37% yield. Cluster **5** exhibits NO stretching absorptions at 1725 and 1699 cm^{-1}. The ^1H NMR spectrum showed equivalent Cp* groups with a single resonance at δ 2.23. The solid-state structure for cluster **5** was determined (see below).

The 62-VSE nitrosyl analog of the 60-VSE Mo/Co/S cubane cluster **2** was prepared by the reaction of $Cp^{Et}{}_2Mo_2S_4$ with 2.1 equiv of $Co(NO)(CO)_3$ in refluxing toluene for 30 min (Scheme 2). Filtration through Celite and subsequent crystallization from a toluene/hexane solvent mixture at −18 °C gave the pure product in 42% yield. Cluster **4a** displayed NO absorptions at 1747 and 1729 cm^{-1} in the IR spectrum, and the ^1H NMR spectrum showed the presence of equivalent Cp^{Et} groups. Elemental analysis and mass spectral analysis also corresponded to the empirical formula for cluster **4a**. The solid-state structure for cluster **4a** was determined and is discussed below. Once again, no reaction occurred at room temperature and diminished yields may be the result of degradation of the $Co(CO)_3NO$ reagent.

A similar cluster, **4b**, can be prepared from the reaction of $Cp_2Mo_2S_2(\mu\text{-}SH)_2$ with 3 equiv of $Co(NO)(CO)_3$ in refluxing toluene for 30 min (Scheme 2). Cluster **4b** exhibited NO absorptions at 1756 and 1726 cm^{-1} in the IR spectrum, and the ^1H NMR spectrum showed the presence of equivalent Cp groups with a single resonance at δ 4.80. The mass spectrum and elemental analysis corresponded to the empirical formula assigned to cluster **4b**, $Cp_2Mo_2Co_2S_4(NO)_2$.

The W analog to cluster **4a** was similarly prepared via the reaction of $Cp^*{}_2W_2S_4$ with 3 equiv of $Co(NO)(CO)_3$ in refluxing toluene for 30 min to give cluster **6**

(26) Sheldrick, G. M. SHELXL-93 Program for Crystal Structure Refinement; University of Gottingen, Gottingen, Germany, 1993.

in 30% isolated yield after crystallization from toluene/hexane at −18 °C (eq 2). Cluster **6** displayed NO

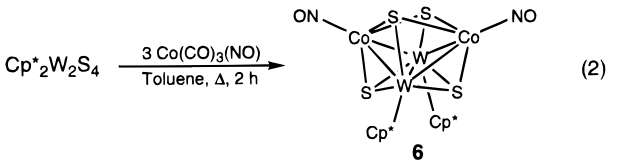

(2)

6

absorptions at 1732 and 1709 cm^{-1} in the IR spectrum, and the ^1H NMR spectrum, with a single resonance at δ 2.09, was indicative of equivalent Cp* groups. The elemental analysis and mass spectrum were consistent with the formula assigned to cluster **6**. The solid-state structure of **6** is presented below.

The tungsten analog to cluster **2** was synthesized in a reaction similar to that for the preparation of **2**.[13e] In this reaction, $Cp^*_2W_2S_4$ reacted with 1 equiv of $Co_2(CO)_8$ in toluene at room temperature to give cluster **7** in high isolated yield (eq 3). Although a crystalline product was

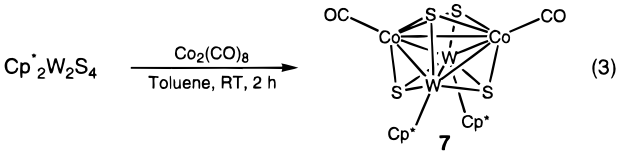

(3)

7

obtained for cluster **7**, which was spectroscopically characterized, an X-ray structural determination was not attempted. Cluster **7** displayed CO absorptions at 1964 and 1946 cm^{-1}, and the ^1H NMR spectrum showed a single resonance at δ 2.13, due to the equivalent Cp* groups. Hydrogen and nitrogen analyses for cluster **7** were consistent with its empirical formula, but the percentage of carbon was low, presumably due to the formation of refractory tungsten carbides.

Another cluster synthon containing only three sulfur atoms, $Cp^{Et}_2W_2S_3(CO)_2$, was used in the attempt to prepare a W analog to cluster **1** by the reaction with 1 equiv of $Co_2(CO)_8$. However, a new type of cluster, **8**, was obtained in 41% isolated yield subsequent to filtration through Celite and crystallization from acetonitrile at −4 °C (eq 4). The IR spectrum for cluster **8**

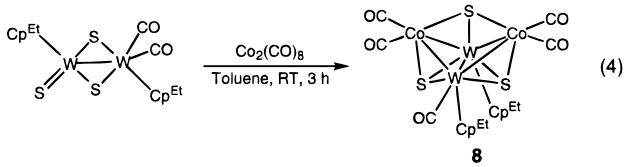

(4)

8

bears a striking resemblance to that for cluster **1**, displaying CO absorptions at 2005, 1981, and 1950 cm^{-1} corresponding to the absorption bands for the CO ligands terminally bound to the Co atoms, and a shoulder at 1924 cm^{-1}, which likely corresponds to the terminal CO on a W atom as revealed by a single-crystal structure determination (see below). The ^1H NMR spectrum was indicative of inequivalent Cp^{Et} ligands that are bisected by a mirror plane of symmetry containing the tungsten atoms. Thus, the ^1H NMR and IR spectra show that the solid-state structure is maintained in solution. As with compound **7**, the percentage of carbon was slightly low, again presumably as a result of tungsten carbide formation during sample combustion.

Table 1. Summary of NO and CO Stretching Vibrations in the IR Spectra (KBr) for 2, 3a, 4a, and 5−8

cluster	νCO or νNO (cm^{-1})
$Cp'_2Mo_2Co_2S_3(CO)_4$ (**1**)	2009, 1984, 1956
$Cp^{Et}_2Mo_2Co_2S_4(CO)_2$ (**2**)	1972, 1950
$Cp^{Et}_2Mo_2Fe_2S_4(NO)_2$ (**3a**)	1736, 1715
$Cp^{Et}_2Mo_2Co_2S_4(NO)_2$ (**4a**)	1747, 1717
$Cp^*_2W_2Fe_2S_4(NO)_2$ (**5**)	1725, 1699
$Cp^*_2W_2Co_2S_4(NO)_2$ (**6**)	1732, 1709
$Cp^*_2W_2Co_2S_4(CO)_2$ (**7**)	1964, 1946
$Cp^{Et}_2W_2Co_2S_3(CO)_5$ (**8**)	2005, 1982, 1952, 1924 (sh)

Structures of the $M_2M'_2S_4X_2$ Clusters (M = Mo, W; M′ = Fe, Co, Ni; X = NO, CO). Selected interatomic distances and angles are collected in Table 2. The table is arranged so that the first three data columns (for **4a**, **6**, and **9**) correspond to clusters with a 62-VSE count, whereas the last three columns contain data for the 60-VSE clusters **3a**, **5**, and **2**. These compounds form a series in which the cluster electron count is varied by changes in the metal atom (M′ = Fe, Co, Ni) or by the vertex ligand (CO or NO).[27,28] Individual features of the structures will be discussed first, followed by a comparison of the main structural changes in the series.

Clusters **4a** and **6** both have crystallographically imposed C_2 symmetry, and the halves of each molecule are related by the transformation $-x + 1, y, -z + {}^1/_2$, but their idealized symmetry is C_{2v}. The Co−Co distances in **4a** and **6** are 3.116(1) and 3.131(1) Å, respectively. These distances are well beyond the typical Co−Co single-bond distance, *cf.* in $Cp'_2Mo_2Co_2S_4(CO)_2$.[6a] These clusters thus consist of a "butterfly" arrangement of metal atoms in the cluster core with five metal−metal bonds. The cobalt atoms occupy the wingtip positions, and the M (M = Mo, W) atoms occupy the hinge positions. The hinge angle between the two M_2Co triangular faces is 81.7(1)° (**4a**) or 81.3(1)° (**6**), compared to 64.6° in **2**. The Mo−Mo and W−W distances in these clusters are very similar, as expected from the similarity of the atomic radii of the Mo and W atoms.[29] All four S atoms are triply bridging in the cluster core, and each caps a face of the metal atom tetrahedron. There are no formal S−S bonds between any of the S atoms in these clusters (S···S distances are all greater than 2.90 Å). In both clusters, the Co−N−O angles are >176°, consistent with terminal, three-electron-donor nitrosyl ligands.[30]

Clusters **3a** and **5** are also isoelectronic and isostructural; cluster **3a** contains a $Mo_2Fe_2(NO)_2$ core, and cluster **5** consists of a $W_2Fe_2(NO)_2$ core. The electron count for both is 60 VSE, corresponding to an electron-precise cluster with 6 metal−metal bonds. Clusters **3a** and **5** have idealized C_{2v} symmetry, although the crystallographically imposed symmetry is C_2 (the halves of each molecule are related by the transformation $-x$

(27) Collman, J. P.; Hegedus, L. S.; Norton, J. R.; Finke, R. G. *Principles and Applications of Organotransition Metal Chemistry*; University Science Books: Mill Valley, CA, 1987.

(28) The electron counting is consistent with the methods described in: (a) Teo, B. K. *Inorg. Chem.* **1984**, *23*, 1251. (b) Teo, B. K.; Longoni, G.; Chung, F. R. K. *Inorg. Chem.* **1984**, *23*, 1257. (c) Lauher, J. W. *J. Am. Chem. Soc.* **1978**, *100*, 5305.

(29) The atomic radius for W is 1.35 Å and for Mo is 1.45 Å: Slater, J. C. *J. Chem. Phys.* **1964**, *41*, 3199.

(30) (a) Elschenbroich, C.; Salzer, A. *Organometallics, A Concise Introduction*, 2nd ed.; VCH: New York, 1992. (b) Enemark, J. H. *Inorg. Chem.* **1971**, *10*, 1952.

Table 2. Selected Interatomic Distances and Angles for the $Cp^{\#}_2M_2M'_2S_4X_2$ Clusters 2, 3a, 4a, 5, 6, and 9

	4a	6	9	3a	5	2[b]
			Atoms			
$M_2M'_2X_2$	$Mo_2Co_2(NO)_2$	$W_2Co_2(NO)_2$	$Mo_2Ni_2(CO)_2$	$Mo_2Fe_2(NO)_2$	$W_2Fe_2(NO)_2$	$Mo_2Co_2(CO)_2$
			Distances			
M−M (M = Mo, W)	2.8135(6)	2.7984(5)	2.829(1)	2.8419(7)	2.8198(9)	2.8313(5)
M′−M′ (M′ = Fe, Co, Ni)	3.116(1)	3.131(1)	2.960(1)	2.7040(11)	2.735(3)	2.5816(9)
av M−M′	2.766(4)	2.780(4)	2.722(2)	2.7654(7)	2.766(4)	2.6931(7)
av M−S_a[c]	2.327(1)	2.328(3)	2.33(1)	2.333(4)	2.327(2)	2.322(3)
M−S_b[c]	2.274(1)	2.269(2)	2.257(7)	2.3199(9)	2.311(2)	2.325(2)
M′−S_a	2.180(1)	2.185(2)	2.160(3)	2.210(1)	2.208(3)	2.175(3)
av M′−S_b	2.260(3)	2.259(43)	2.283(4)	2.228(1)	2.243(6)	2.213(6)
av M′−N	1.636(3)	1.635(6)		1.668(3)	1.659(9)	
			Angles			
av M′−N−O	176.2(4)	178.2(6)		179.0(3)	175.0(9)	
av M−S−M	74.31(3)	73.87(4)	74.82(8)	75.03(3)	74.59(7)	75.1(1)
av M−S−M′	75.4(3)	75.6(4)	74.1(5)	74.90(3)	75.0(2)	73.2(4)
av M′−S−M′	87.17(4)	86.48(6)	80.9(1)	74.70(4)	75.13(9)	71.34(2)

[a] Calculated from the data in ref 6c. [b] Calculated from the data in ref 6a. [c] $S_a = \mu_3$-S atoms on the MMM′ faces; $S_b = \mu_3$-S atoms on the M′M′M faces.

Table 3. Summary of Crystallographic Data for 3a, 4a, and 5

	3a	4a	5
empirical formula	$C_{22}H_{34}N_2O_2S_4Fe_2Mo_2$	$C_{22}H_{34}N_2O_2S_4Co_2Mo_2$	$C_{20}H_{30}N_2O_2S_4Fe_2W_2$
fw	790.33	796.49	938.10
cryst color and habit	black, irregular	black plate	black plate
cryst dimens, mm	0.12 × 0.22 × 0.24	0.14 × 0.26 × 0.28	0.06 × 0.12 × 0.24
cryst syst	monoclinic	monoclinic	monoclinic
space group	*C*2/*c* (No. 15)	*C*2/*c* (No. 15)	*C*2/*c* (No. 15)
a, Å	20.928(3)	21.362(3)	20.727(4)
b, Å	8.757(1)	8.588(2)	8.865(1)
c, Å	16.387(2)	16.610(3)	16.593(3)
β, deg	109.988(5)	111.38(1)	120.46(1)
V, Å^3	2822.3(6)	2837.5(9)	2628.1(8)
Z	4	4	4
density (calcd), g cm^{-3}	1.860	1.86_4	2.37_1
F(000), e	1584	1592	1776
linear abs coeff (*μ*), cm^{-1}	21.95	23.30	101.46
scan type	*ω* scan	*ω* scan	*ω* scan
2*θ* scan range, deg	5−52	5−52	5−52
octants used	$+h,+k,\pm l$	$+h,+k,\pm l$	$+h,+k,\pm l$
scan rate, deg min^{-1}	2−20, variable	2−20, variable	2−20, variable
scan width, deg	0.6 below Kα_1 to 0.6 above Kα_2	0.6 below Kα_1 to 0.6 above Kα_2	0.9 below Kα_1 to 0.9 above Kα_2
bkgd/scan ratio	0.5	0.5	0.5
no. of data collected	3625	3773	3476
no. of unique rflns	2771, $R_{int} = 0.0455$	2793	2581
relative max/min transmissn	1.260/0.693	1.231/0.837	1.387/0.795
no. of data/restraints/params	2768/0/223	2793/0/169	2571/0/151
final *R* indices ($I \geq 2\sigma(I)$)	R1 = 0.0383, wR2 = 0.1051	R1 = 0.0305, wR2 = 0.0858	R1 = 0.0376, wR2 = 0.0910
R indices (all data)	R1 = 0.0401, wR2 = 0.1063	R1 = 0.0351, wR2 = 0.0879	R1 = 0.0561, wR2 = 0.0965
GOF	1.083	1.093	0.940
mean shift/error	<0.001	<0.001	<0.001
max shift/error	<0.001	<0.001	<0.001
secondary extinction	0.0009(2)	3 rflns excluded from refinement	no cor applied
residual electron density, e Å^{-3}	+1.17/−1.95	+0.977/−0.861	+1.783/−2.459

+ 1, *y*, −*z* + $^1/_2$). The four metal atoms in these clusters, M_2Fe_2 (M = Mo, W), form a completely metal−metal-bonded tetrahedron. There are no S−S bonds, as all S···S distances are greater than 2.90 Å. The Fe−Fe single-bond distances, 2.7040(1) and 2.735(3) Å in **3a** and **5**, respectively, are slightly longer (*ca.* 0.1 Å), but comparable to, the conventional Fe−Fe single-bond distance found in other similar clusters.[31] Each S atom is triply bridging and caps a face on the M_2Fe_2 core, and the (μ_3-S)−Fe and (μ_3-S)−M distances are as expected.[6,13,14] The Fe−N−O angles are >175°, consistent with terminal, three-electron-donor NO ligands.[30]

Aside from the elongation of the Co···Co distance, the core structures of **4a** and **6** change minimally relative to cluster **2**, and the observed changes appear for the most part to be reorganizations to accommodate the increase in the Co···Co distance. In clusters **4a** and **6**, the (μ_3-S)−M distances to the S atoms that cap the M−M−Co faces are 2.3267(9) Å (**4a**) and 2.328(3) Å (**6**). The (μ_3-S)−M interatomic distances corresponding to the S atoms which cap the open Co−Co−M faces are 2.2741(10) Å (**4a**) and 2.269(2) Å (**6**). Relative to cluster **2**, the changes associated with the (μ_3-S)−Co distance in **4a** are the slight expansion of the (μ_3-S)−Co distances in the Co−Mo−Mo faces (2.180(1) Å), compared with 2.175(3) Å in **2**, and the elongation in the (μ_3-S)−Co distance at the Co−Co−Mo face (2.260(3) Å) compared with 2.213(6) Å in **2**. These distance increases are consistent with the expansion of the Co···Co distance.

(31) (a) The Fe−Fe distance in $Fe_4(NO)_4(\mu_3\text{-S})_4$ is 2.634(1) Å: Gall, R. S.; Chu, C. T.-W.; Dahl, L. F. *J. Am. Chem. Soc.* **1974**, *96*, 4019. (b) The Fe−Fe distance in $Cp'_2V_2Fe_2S_4(NO)_2$ is 2.590(1) Å: Bolinger, C. M.; Weatherill, T. D.; Rauchfuss, T. B.; Rheingold, A. L.; Day, C. S.; Wilson, S. R. *Inorg. Chem.* **1986**, *25*, 634.

Table 4. Summary of Crystallographic Data for 6 and 8

	6	**8**
empirical formula	$C_{20}H_{30}N_2O_2S_4Co_2W_2$	$C_{27}H_{34}O_5S_3Co_2W_2$
fw	944.26	1020.28
cryst color and habit	black needle	black plate
cryst dimens, mm	0.36 × 0.07 × 0.06	0.08 × 0.18 × 0.22
cryst syst	monoclinic	monoclinic
space group	*C*2/*c* (No. 15)	$P2_1/n$ (No. 14)
a, Å	21.007(2)	11.271(1)
b, Å	8.738(1)	21.283(2)
c, Å	16.821(1)	12.757(1)
β, deg	120.45(1)	91.218(7)
V, Å^3	2661.8(4)	3059.4(5)
Z	4	4
density (calcd), g cm^{-3}	2.35$_6$	2.215
F(000), e	1784	1944
linear abs coeff (μ), cm^{-1}	101.74	88.00
scan type	ω scan	ω scan
2θ scan range, deg	5−52	5−52
octants used	$+h,+k,\pm l$	$+h,+k,\pm l$
scan rate, deg min^{-1}	4−20, variable	5−20, variable
scan width, deg	0.6 below Kα_1 to 0.6 above Kα_2	0.7 below Kα_1 to 0.7 above Kα_2
background/scan ratio	0.5	0.5
no. of data collected	3402	7534
no. of unique rflns	2599	6005
rel max/min transmissn	1.175/0.661	1.227/0.681
no. of data/restraints/params	2598/0/152	5999/0/363
final *R* indices ($I \geq 2\sigma(I)$)	R1 = 0.0249, wR2 = 0.0550	R1 = 0.0322, wR2 = 0.0709
R indices (all data)	R1 = 0.0398, wR2 = 0.0578	R1 = 0.0475, wR2 = 0.0737
GOF	0.797	0.935
mean shift/error	<0.001	<0.001
max shift/error	<0.001	<0.001
secondary extinction	0.00014(2), plus 1 rfln excluded	no cor applied
residual electron density, e Å^{-3}	+1.464/−0.685	+1.852/−0.977

Bonding in the Cubane Clusters. The structures of the cubane type clusters with an $M_2M'_2S_4$ core may be discussed in terms of the 18-electron rule or in terms of an EHMO scheme.[32] The premise that an M_4 cluster with 60 VSE will have 6 metal−metal bonds rests upon the 18-electron rule: 4 metals with 18 electrons each requires 72 VSE total, but 2 electrons must be subtracted for each metal−metal bond, as these elecrons are counted twice (once for each bonded metal). Hence, 12 electrons must be subtracted for an M_4 cluster with 6 metal−metal bonds. Implicit in this scheme is the assumption that a set of formal oxidation states may be assigned to the metal atoms in the cluster such that *each* metal achieves the 18-elecron count, as opposed to a global count that satisfies a delocalized bonding scheme as, for example, in an EHMO scheme.

In the cubane type clusters represented by the compounds listed in Table 2, a unique set of oxidation states may be assigned to the metal atoms if it is assumed that each of the μ_3-S ligands (oxidation state 2−) contributes 2 electrons to each of the 3 metal atoms to which it is bonded. Then, the formal oxidation states of the metals in the 62-VSE nitrosyl clusters are M(III) and Co(I) (the nitrosyl ligand is assumed to be NO^+). The formal oxidation states in the 62-VSE carbonyl cluster **9** are Mo(III) and Ni(II). In the 60-VSE clusters

(32) Harris, S. *Polyhedron* **1989**, *8*, 2843.

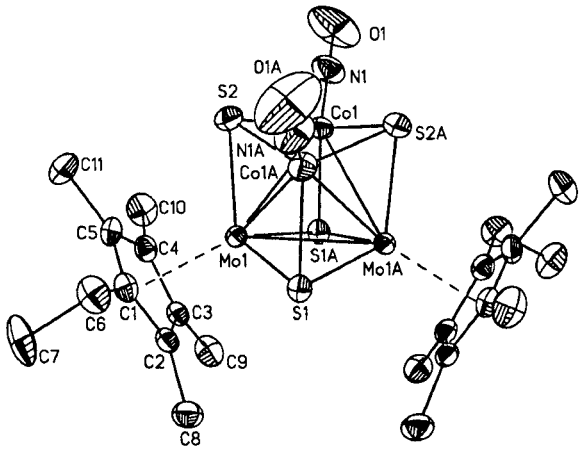

Figure 1. ORTEP plot of $Cp^{Et}{}_2Mo_2Co_2S_4(NO)_2$ (**4a**) with the atomic numbering scheme. Thermal ellipsoids are drawn at the 50% probability level.

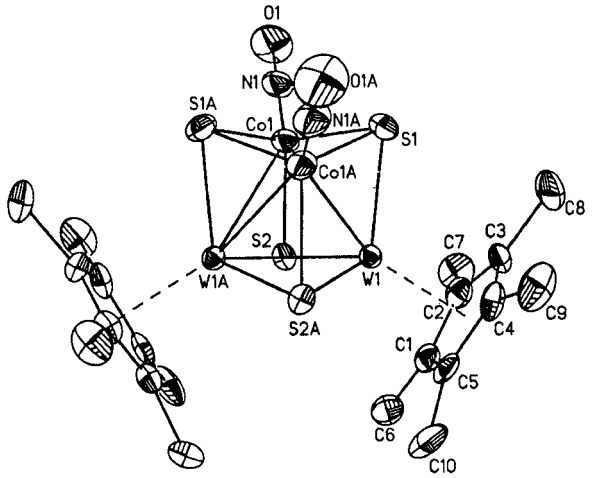

Figure 2. ORTEP plot of $Cp^*{}_2W_2Co_2S_4(NO)_2$ (**6**) with the atomic numbering scheme. Thermal ellipsoids are drawn at the 50% probability level.

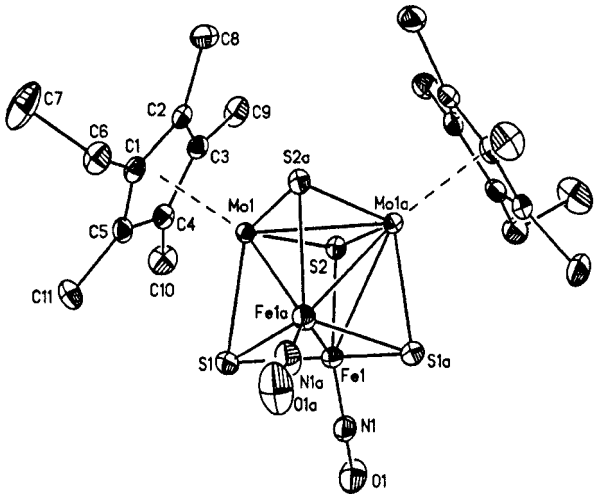

Figure 3. ORTEP plot of $Cp^{Et}{}_2Mo_2Fe_2S_4(NO)_2$ (**3a**) with the atomic numbering scheme. Thermal ellipsoids are drawn at the 50% probability level.

3a, **5**, and **2**, the corresponding oxidation states are M(III) and Fe(I) or Mo(III) and Co(II). Thus, in a formal sense, all the changes in the electron count involve the M′ (first transition row) metal atoms. This conclusion rests on the experimentally determined structure, however, as we arrive at the oxidation states by a knowledge

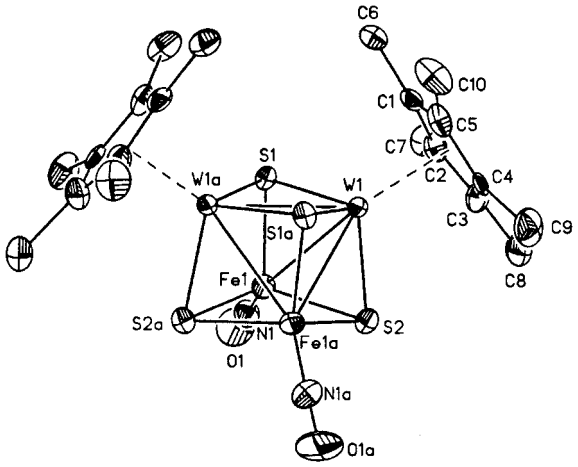

Figure 4. ORTEP plot of $Cp^*_2W_2Fe_2S_4(NO)_2$ (**5**) with the atomic numbering scheme. Thermal ellipsoids are drawn at the 50% probability level.

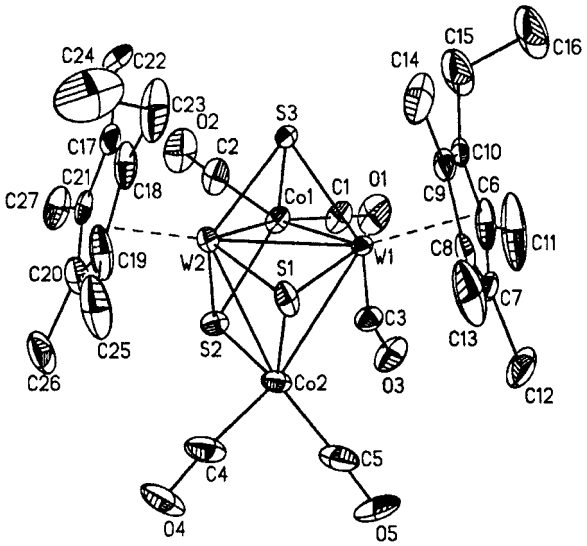

Figure 5. ORTEP plot of $Cp^{Et}_2W_2Co_2S_3(CO)_5$ (**8**) with the atomic numbering scheme. Thermal ellipsoids are drawn at the 50% probability level.

of which metal pairs are bonded and which are not. *A priori*, any one of the metal−metal bonds could be broken on going from the 60-VSE cluster to its 62-VSE cousin, and a different set of formal oxidation states would be assigned accordingly.

Harris has calculated the EHMO energy level scheme for this $M_2M'_2S_4$ type of cluster and finds that a cluster metal electron count of 20 is necessary for a completely bonded metal tetrahedron.[32] Of these 20 electrons, eight occupy low-energy, ligand-centered orbitals, leaving 12 electrons to occupy the metal−metal bonding orbitals. Metal electrons in excess of 20 occupy metal−metal antibonding orbitals. The metal oxidation states assigned above are consistent with this scheme. In **3a**, **5**, and **2**, each Fe or Co atom contributes 7 electrons and each M atom contributes 3 electrons to the cluster, giving a total of 20 electrons available to occupy the metal-based cluster orbitals and giving rise to a completely bonded tetrahedron of metal atoms, as indicated by the metal−metal interatomic distances in these clusters. In clusters **4a**, **6**, and **9**, the metal oxidation states assigned above give a total of 22 electrons available to occupy the metal-based cluster orbitals. The occupation of all 6 metal−metal bonding orbitals and 1 metal−metal antibonding orbital is consistent with the presence of 5 metal−metal bonds in these clusters, as indicated by the metal−metal distances. The electron count in clusters **4a**, **6**, and **9** is related to those in clusters **3a**, **5**, and **2** by an addition of 2 electrons to the metal−sulfido core effected by the replacement of 2 metal atoms with metal atoms one group to the right in the periodic table or by the effective addition of 2 electrons by the replacement of the CO ligands (2e donor) with NO ligands (3e donor). In either case, the result is cleavage of the M′−M′ bond. This suggests that the LUMO in these $M_2M'_2S_4$ clusters has considerable σ^*(M′−M′) character. If the M′−M′ bond is the weakest of the metal−metal bonds in the cluster (as anticipated), then the HOMO would have σ(M′−M′) character and, most likely, σ^*(M′−M′) as the LUMO. This conclusion was also reached on the basis of the structural effects of reduction or oxidation of the 60-VSE cluster **2**.[5a,6a,33,34]

Practically all the structural changes seen in the series of clusters listed in Table 2 can be attributed to the geometrical responses of the "cubes" to the elongation of the M′−M′ distance in the 62-VSE clusters compared to their 60-VSE counterparts. The hinge angles between the MMM′ faces open up to ca. 81° as opposed to 65° in the 60-VSE clusters. There is a corresponding increase in the M′−S−M′ angle, from ca. 75 to 87° on going from the 60- to 62-VSE clusters, and the M′−S_b distances are stretched by about 0.04 Å. This stretching of the M′−S bond apparently leaves the S_b ligand free to bind more strongly to the early transition metal: the M−S_b distance shrinks by about 0.05 Å.

Structure of Cluster 8. Efforts to synthesize an electron-deficient trisulfido nitrosyl cluster with a core geometry similar to that found in **1** were unsuccessful in all attempts using the cluster synthon $Cp_2Mo_2S_2(\mu\text{-}SH)_2$ (from which **1** is prepared). Therefore, the tungsten dimer $Cp^{Et}_2W_2S_3(CO)_2$ was used in the effort to obtain a cluster with a core structure containing 4 metal atoms and 3 sulfur atoms. The resultant product, cluster **8** (shown in Figure 5), has no crystallographically imposed symmetry but does have idealized C_s symmetry with the mirror plane containing the W−W bond. The cluster consists of a butterfly arrangement of metal atoms with W at the hinge positions and Co at the wingtips. The hinge angle between the two W_2Co triangular faces is 80.5(1)°, and the Co···Co distance is nonbonding (>3.2 Å).

This structure represents yet another way of achieving the saturated 62-VSE count for 5 metal−metal bonds: the addition of an "extra" 2-electron-donor ligand (the 5th CO group). The sulfur atoms are all triply bridging; two of them cap the "closed" W_2Co faces, and the third caps the "open" Co_2W face. The most notable feature of this cluster, however, is the terminal CO ligand bound to the W atom. Conceptually, cluster **8** represents the addition of a CO ligand to the W analog of cluster **1**, in which the added CO ligand is bonded to one of the W atoms. In contrast, the addition of Me_3P, or CO under high pressure, to cluster **1** results in an adduct in which the added ligand is bonded to the wingtip cobalt atom rather than to the hinge atom as

(33) Curtis, M. D.; Druker, S. H.; Goossen, L.; Kampf, J. W. *Organometallics*, in press.
(34) Mansour, M. A.; Curtis, M. D.; Kampf, J. W., to be submitted for publication.

Table 5. Summary of Cyclic Voltammetry for Clusters 2, 3a, 4a, 5, 6, and 8

compd	$E'_{p,red}$ (mV)	ΔE_p (mV)	$i_{p,a}/i_{p,c}$	$E'_{p,ox}$ (mV)	ΔE_p (mV)	$i_{p,c}/i_{p,a}$
$Cp^{Et}{}_2Mo_2Co_2S_4(CO)_2$ (**2**)	−1042	81	0.9	197	154	0.4
				621		
$Cp^{Et}{}_2Mo_2Fe_2S_4(NO)_2$ (**3a**)	−722	90		617	224	
	−1118	82		1001		
	−1457	95		1299	224	
$Cp^{Et}{}_2Mo_2Co_2S_4(NO)_2$ (**4a**)	−1526	68	0.9	195	74	0.7
				978		
				1328	207	
$Cp^*{}_2W_2Fe_2S_4(NO)_2$ (**5**)	−1316	79		480		
	−1493	61		792	108	
	−1931	110		1535	246	
$Cp^*{}_2W_2Co_2S_4(NO)_2$ (**6**)	−1750	69	0.8	71	61	0.8
				846		
				1330	217	
$Cp^{Et}{}_2W_2Co_2S_3(CO)_5$ (**8**)	−1111	78	1.0	161		
	−1713	79	0.9	554		
	−2227	190	0.6	693	166	
				880	63	
				1044	70	

in **8**.[5d,35] With cluster **1**, the addition of these ligands is reversible and the adducts revert to **1** under reduced concentration of ligand. The preference of the CO to bind to W in **8** may be related to the greater ease of oxidation of W as oppposed to Mo. The W−C−O angle in **8** is *ca*. 162°, which suggests some interaction of the CO group with the wingtip metal atoms as was observed in the butterfly cluster $Cp'_2Mo_2Fe_2S_2(CO)_8$.[6c] However, the closest CO···cluster atom distance is >3.6 Å; thus, any interaction, if present at all, must be very weak.

Cyclic Voltammetry of Clusters 2, 3a, 4a, 5, 6, and 8. Metal sulfur clusters possess a remarkable degree of stability to multiple oxidation states. This is largely due to the polarizable orbitals of the S atoms[36] and the Cp^- ligands which are electron donating, thereby making reductions more difficult and imparting stability for cations;[8] in many cases, the HOMOs and LUMOs are only weakly metal−metal bonding or antibonding, respectively.[37] Stereochemical consequences of electron addition and removal can be physically observed, and these experimental data can serve to corroborate theoretical descriptions of the bonding in these types of compounds.[38] Experimental work on the reduction[33] and oxidation[5a,34] of the cubane cluster **2** and the qualitative MO studies by Harris[32] on "$M_2M'_2S_4$" clusters and by Dahl[39] and Curtis[37] on the analogous "M_4S_4" clusters indicate that reduction of the bimetallic sulfido cluster compounds results in the filling of predominantly metal−metal antibonding orbitals, while oxidation results in the removal of electrons from predominantly metal−metal bonding orbitals.[40] We have examined the redox chemistry of clusters **2**, **3a**, **4a**, **5**, **6**, and **8**, and a summary of the electrochemical data is in Table 5.

The cyclic voltammograms of the nitrosyl $M_2Co_2S_4$ (M = Mo, W) clusters **4a** and **6** are similar. Cluster **4a** undergoes a single one-electron reversible reduction at $E_{p,red1} = -1526$ mV, and cluster **6** undergoes a single reduction at $E_{p,red2} = -1750$ mV. The peak separation values for these reductions were comparable to the ΔE_p value for the Fc/Fc^+ reference couple, a reversible, one-electron transfer process, under identical conditions.[24a] Tungsten complexes are known to undergo more facile oxidation processes and more difficult reduction processes than their Mo analogs,[41] and these data are consistent with this behavior. The carbonyl analog **2** undergoes a single, reversible, one-electron-reduction process as well. However, the reduction potential for this process (−1042 mV) is significantly lower than the reduction potentials for **4a** and **6**. This indicates that the LUMO in **2** and, in fact, in all the 60-VSE clusters is lower in energy than those in **4a**, **6**, and other 62-VSE clusters.

Cluster **6** undergoes a reversible, one-electron oxidation at $E_{p,ox1} = 71$ mV, followed by a second oxidation which is irreversible ($E_{p,ox2} = 846$ mV). Subsequent to the second oxidation process, it appears that surface adsorption on the electrode and oxidation processes are occurring. The peak currents become very large relative to the reversible redox couples, indicative of the formation of an electroactive coating on the electrode.[42] Continuous scanning of these samples results in the appearance of a reduction peak at $E_{p,red} = 458$ mV, which is absent when the potential scan is reversed before the third oxidation step occurs.

The analogous processes are seen for cluster **4a**, except at higher potentials. A one-electron oxidation at $E_{p,ox1} = 195$ mV was observed. Subsequent to the first reversible oxidation step, there is an irreversible oxidation followed by a third oxidative electron transfer at $E_{p,ox3} = 1328$ mV. The last oxidation appears to be quasi-reversible with an apparent re-reduction at $E_{p,red} = 1121$ mV. For comparison, the 62-VSE carbonyl cluster $Cp'_2M_2Ni_2S_4(CO)_2$ (**9**) undergoes two one-electron reductions at $E_{p,red} = -1610$ and −2140 mV and two irreversible oxidations at −110 and +90 mV.[6c] It appears, then, that the nitrosyl clusters are only slightly more easily reduced, but considerably more difficult to oxidize, than their carbonyl analogs with the same cluster electron count. Apparently the nitrosyl ligand, relative to CO, lowers the energy of the HOMO by stronger π-back-bonding, but the energy of the LUMO is much less affected.

For the 60-VSE cluster **3a**, two successive, reversible reduction processes ($E_{p,red1} = -722$ mV and $E_{p,red2} = -1118$ mV) precede a third reduction step at $E_{p,red3} = -1457$ mV, which appears to be quasi-reversible. For cluster **5**, similar behavior is seen, except the reduction potentials are more negative. The first reversible reduction wave is seen at $E_{p,red1} = -1388$ mV, followed by a second reversible reduction at $E_{p,red2} = -1493$ mV. The third, "quasi-reversible" step occurs at $E_{p,red3} = -1931$ mV.

The oxidation processes for clusters **3a** and **5** are more complex. Cluster **3a** undergoes an initial, irreversible oxidation process at $E_{p,ox1} = 617$ mV. Two successive, irreversible oxidation processes occur at $E_{p,ox2} = 1001$ mV and $E_{p,ox3} = 1299$ mV. Cluster **5** undergoes analo-

(35) Curnow, O. J.; Kampf, J. W.; Curtis, M. D.; Mueller, B. L. *Organometallics* **1992**, *11*, 1984.
(36) Meyer, T. J. *Prog. Inorg. Chem.* **1975**, *19*, 1.
(37) Williams, P. D.; Curtis, M. D. *Inorg. Chem.* **1986**, *25*, 4562.
(38) (a) Zanello, P. *Struct. Bonding* **1992**, *79*, 101. (b) Zanello, P. *Coord. Chem. Rev.* **1988**, *87*, 1.
(39) Chu, C. T.-W.; Lo, F. Y.-K.; Dahl, L. F. *J. Am. Chem. Soc.* **1982**, *104*, 3409 and references therein.
(40) Davies, C. E.; Green, J. C.; Kaltsoyannis, N.; MacDonald, M. A.; Qin, J.; Rauchfuss, T. B.; Redfern, C. M.; Stringer, G. H.; Woolhousse, M. G. *Inorg. Chem.* **1992**, *31*, 3779.
(41) Honrath, U.; Vahrenkamp, H. *Z. Naturforsch.* **1984**, *39B*, 545.
(42) Bard, A. J.; Faulkner, L. R. *Electrochemical Methods: Fundamentals and Applications*; Wiley: New York, 1980.

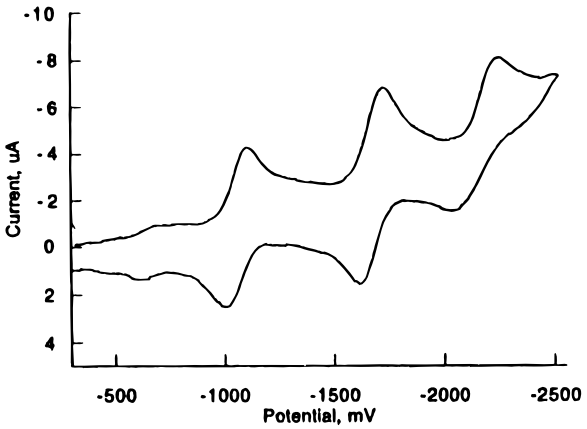

Figure 6. Cyclic voltammogram $Cp^{Et}{}_2W_2Co_2S_3(CO)_5$ (**8**) in CH_3CN (scan rate 200 mV/s).

gous, complex oxidations with the first irreversible oxidation process at $E_{p,ox1} = 480$ mV, followed by two successive oxidations at $E_{p,ox2} = 792$ mV, which is irreversible, and $E_{p,ox3} = 1535$ mV, which appears to be "quasi-reversible", with a re-reduction at $E_{p,red} = 1289$ mV. The current responses for these oxidations are also much larger than those observed for the reversible reduction waves, again indicating the formation of electroactive surface deposits.

Cluster **8** undergoes several facile reductions which appear to be uncomplicated (Figure 6). The first reversible reduction occurs at $E_{p,red1} = -1111$ mV. This is followed by a second, reversible reduction at $E_{p,red2} = -1713$ mV. A third, "quasi-reversible" reduction occurs at $E_{p,red3} = -2227$ mV and the reverse re-oxidation occurs at $E_p = -2037$ mV ($\Delta E_p = 190$ mV). The oxidation processes for cluster **8** are more complex, as found for clusters **3a** and **5**. An initial irreversible oxidation process is seen at $E_{p,ox1} = 161$ mV and is followed by four successive oxidation processes as a result of the formation of one or more new chemical species that undergo the oxidation processes at higher potentials.

A summary of the IR data for clusters **1**, **2**, **3a**, **4a**, and **5**−**8** is given in Table 1. A comparison of the spectra of the Mo clusters with their W analogs shows, in all cases, that ν_{NO} *or* ν_{CO} values are lower for the W clusters. Thus, the π-acceptor ligands receive enhanced back-donation in the W clusters, which are effectively more "electron rich". The cyclic voltammograms of these clusters revealed that the W clusters undergo more facile oxidations than their Mo analogs, which is also consistent with the W clusters being more electron rich.

Conclusions

The rational syntheses of a series of heterobimetallic sulfido nitrosyl clusters are reported. X-ray structure determinations of the clusters show that their core geometries are consistent with theoretical bonding schemes for clusters obeying the 18-electron rule and that the HOMO and LUMO of the $Cp_2M_2M'_2S_4L_2$ clusters are σ(M′−M′) and σ*(M′−M′), respectively. The electrochemistry of these clusters shows that they have multiple, stable oxidation states and that, in comparison with isostructural carbonyl clusters, the nitrosyl ligand depresses the energy of the HOMO relative to the LUMO. The 60-VSE clusters are reduced at more positive potentials than the corresponding 62-VSE clusters, suggesting that the energy of the LUMO in the former is at a lower energy.

Acknowledgment. We are grateful for the support furnished by the National Science Foundation (Grants CHE-9205018 and CHE-9523056).

Supporting Information Available: Tables of data collection parameters, bond lengths, bond angles, fractional atomic coordinates, anisotropic thermal parameters, and hydrogen atom fractional coordinates for **3a**, **4a**, **5**, **6**, and **8** (31 pages). Ordering information is given on any current masthead page.

OM960724C